DECOVALEX 2015

Project: THM behaviour of bentonite and sand-bentonite materials: Numerical simulation of two laboratory column experiments

Author und Co-author(s)	Dr. Ballarini E., Prof. Dr. Bauer S.
Institution	Institute for Geoscience University of Kiel
Address	Ludewig-Meyn-Str. 10, 24118 Kiel, Germany
Telephone, E-mail, Internet address	ballarin@gpi.uni-kiel.de/ sebastian.bauer@gpi.uni-kiel.de
Duration of the Project	November 2013 – December 2015

ABSTRACT

The present report summarizes the work carried out by the University of Kiel on a part of the Task B1 for the DECOVALEX 2015 project, which compares and benchmarks numerical models and complex coupled simulations of radioactive waste disposal related processes. Aim of Task B1 is to understand the Thermo-Hydro-Mechanical (THM) processes taking place in a disposal system of high level radioactive waste (HLRW) in the early post closure period, through the analysis of well controlled in situ and laboratory experiments. The performance of deep geological repositories of HLRW is influenced by the utilized buffer materials. In general, bentonite and sand bentonite mixtures are planned to seal the area around the canister, because of their thermal-hydro-mechanical properties. This sealing layer around the canisters experiences an initial drying due to the heat produced by HLRW and a successive re-saturation with fluid from the host rock. These complex thermal, hydraulic and mechanical processes were investigated in two laboratory column experiments using firstly MX-80 clay pellets and secondly a mixture of 35% bentonite and 65% sand. These experiments are part of PEBS project and were performed in the CIEMAT laboratories in Madrid.

In this study, we aim to 1) identify and understand the most relevant processes taking place in the buffer materials; 2) identify and quantify the key physical parameters that determine the material behavior under heating and hydrating conditions. Therefore, a fully coupled and process-oriented 2D numerical model was applied to validate the experiments, simulate the heat transport, multiphase flow and mechanical effects from swelling and thermal expansion. As both experiments were performed with a similar experimental set-up, the thermal parameters of the insulations and the heater device were kept unchanged in the two models, while the parameters of the buffer material were fitted during model calibration. A good fit between the model results and the data was achieved for temperature, relative humidity, water intake and swelling pressure. The key variables identified by the model are the permeability and relative permeability, the water retention curve and the thermal conductivity of the buffer materials.

Project goals

An important part of the performance and safety assessment of disposal systems for radioactive waste and spent nuclear fuel in deep geological formations is to evaluate the impact on repository performance of the coupled effects of mechanical deformation, fluid and gas flow through the repository as well as thermal loading from the decaying waste. In this context, the DECOVALEX project (DEvelopment of COupled models and their VALidation against Experiments; http://www.decovalex.org) is an international research and model comparison collaboration, initiated in 1992, for advancing the understanding and modeling of coupled thermo-hydro-mechanical (THM) and thermo-hydro-mechanical-chemical (THMC) processes in geological systems. The project has been conducted by research teams supported through a large number of radioactive-waste-management organizations and regulatory authorities working on selected modeling test cases, followed by comparative assessment of model results. Currently, modeling teams from ten international partner organizations participate in the comparative evaluation of five modeling tasks involving complex field and/or laboratory experiments.

The work carried out by the University of Kiel in support of ENSI focuses on the numerical simulation of two laboratory column experiments performed within Task B1 of the DECOVALEX 2015 project and the PEBS FP7 EU project (www.pebs-eu.de). The final objective of Task B1 is the numerical simulation of the HE-E in situ heating experiment performed in a tunnel in the Mont Terry laboratory to improve the understanding of the thermal evolution of the near field around a high level waste (HLW) canister during the early phase after emplacement [1] [2] [3]. The experiment consists of two tunnel sections with heaters, which represent the waste canisters. One section is filled using pure MX80 bentonite pellets while the other section is filled using a 35% MX-80 bentonite and 65% quartz sand mixture. This report describes the numerical simulation of two well controlled laboratory THM column experiments designed to test the backfill materials and mimic the expected field conditions of heating and hydration expected to take place in the tunnel experiment HE-E.

In the HE-E experiment, after the emplacement of the canister, the buffer material is heated while in the later stages the circulation of water coming from the Opalinus clay host rock will saturate the buffer. Therefore, also in the laboratory experiments, these processes are reproduced and the experiments are divided into 1) a heating phase and 2) a heating and hydration phase. A heater positioned at the bottom of the columns applied heat. The heating phase is characterized by a stepwise increase of the temperature at the heater plate from 100 °C to 140 °C, which is the expected maximum temperature reached in the area surrounding the canister [4]. The resaturation with water is reproduced using a hydration line positioned at the top of the cells, which allows the injection of water having composition similar to the pore water in the Opalinus Clay formation.

Our work aimed: 1) to identify the most relevant processes in the buffer materials and 2) to quantify the key physical parameters determining the material behavior under heating and hydrating conditions. These aims were pursued by developing a fully coupled 2D numerical model of the experiments, simulation of heat transport, multiphase flow and mechanical effects from swelling and thermal expansion and by subsequent parameter identification. The modelling results contribute to provide reliable quantitative parameters for the two buffer materials, which can then be applied for the in-situ field-scale HE-E experiment.

Work carried out and results obtained

The experimental set-up is described in detail in [4] and [5], here only a short summary is provided to better understand the modelling work. The materials tested in the column experiments, and parameterized using numerical simulations in this study, are the same as those used as buffer in the two sections of the HE-E field experiment [4] [5]. The bentonite filling one column was in the form of granulate (pellets), while the sand-bentonite mixture is constituted of 65% quartz sand (diameter ranging from 0.5 to 1.8 mm) and 35% Na-bentonite GELCLAY WH2 [4]. The internal diameter of the column is around 7 cm and its height 50 cm. In both columns, the heating system consists of two steel plates (316L stainless steel) inserted at the bottom of the cell with a resistance sandwiched between the plates (Fig. 1b and c). The lower plate is insulated, while the upper one is treated with a conductive paste to better transmit the heat to the filling material. The

power provided to the resistance is adjusted to match the desired temperature on the upper heater plate. The top of the filling material is closed by a porous stone and by a plug, which is connected to a cooling system (Fig. 1a) that maintains the temperature on the upper part at the laboratory temperature, while during the hydration phase it allows the infiltration of a sodium-rich solution at laboratory temperature. The column of Exp-B is equipped with a load cell between the hydration piece and the upper plate with the aim of measuring the swelling pressure during the test.

The cells are instrumented with temperature, relative humidity, water intake and (only for B-Exp) axial load cell. Temperature (T) and relative humidity (RH) were measured at Sensor1, Sensor2 and Sensor3 (placed inside the filling material at 10, 22 and 40 cm from the heater plate as shown in Fig. 1a, b and c), while temperature was additionally monitored inside the insulation (Teflon) and on the top of the heater plate (Fig. 1a–c). The heater power supplied was measured during the experiments and adjusted to maintain the desired heater temperature. Water intake was measured through the weight loss of the water deposits (Fig. 1a). For Exp-B, where high swelling of the material was expected, the axial pressure generated during the hydration phase was recorded at the load cell at the top of the column (Fig. 1b).

Once RH and T were stable (stabilization phase of the experiment where no power was supplied to the heater), the heating phase of the experiments started and these parameters were constantly monitored until the end of the experiments. Initially, the power supplied to the heater allowed reaching a temperature of 100 °C at the top of the heater plate in both cells (until 3524 h in Exp-B and 2498 h in Exp-SB). Successively, the power supplied was increased in order to reach a temperature of 140 °C maintained until the end of the experiments.

Model set-up

The main thermal-hydraulic processes expected to occur in the Exp-B and Exp-SB during the test are: a) heating of the buffer material, lateral heat transport through the insulation material and hydration of the buffer material by water infiltration from the top of the column during the hydration phase. Only for Exp-B mechanical effects due to the swelling pressure are considered. A complete formulation of the balance equations, constitutive models

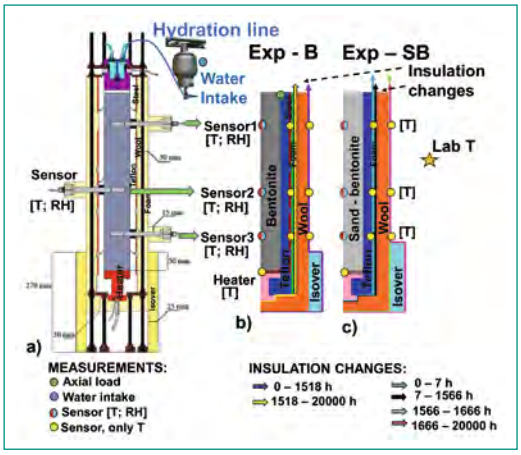

Figure 1:
(a) Full experimental set-up for Exp-B (modified from [4]); (b) simplification of the Exp-B showing the different materials, the points of measurement and the changes in the insulation; (c) simplification of the Exp-SB showing the different materials, the points of measurement and the changes in the insulation.

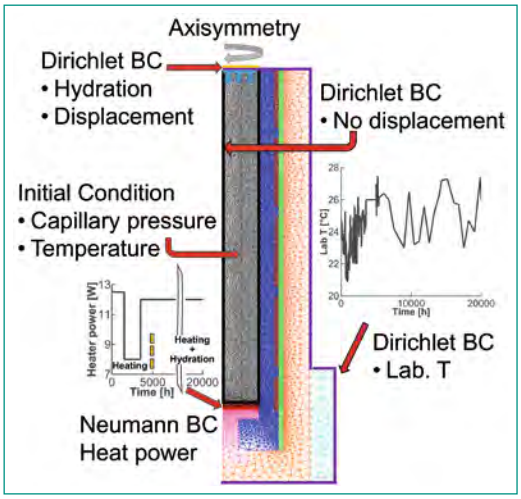

Figure 2:
Model set-up for Exp-B, including the boundary conditions of laboratory temperature and the heater power supplied.

and equilibrium restrictions used can be found in [9]. To analyze the coupled THM processes, a porous medium approach with the three phases solid, liquid and gas is used. Simulations are performed using the scientific open source code OpenGeoSys [6] [7] [8].

A 2D radially symmetric model (OpenGeosys) was set up for the bentonite column (Bastian Graupner) and it was extended for the sand-bentonite mixture (Elisabetta Ballarini) (Fig. 2). The model accounts for the different materials used in the experiment (Fig. 1b and c) i.e., bentonite and sand-bentonite mixture, Teflon, insulation foam, insulation wool, isover, stainless steel shells in case of the Exp-B and the upper and lower heater devices.

As initial conditions (IC), a suction value of 109 MPa (RH of around 45 %) was applied to the bentonite in the Exp-B case. For the Exp-SB column, suction is 106 MPa initially (RH of 46 %), which is reduced in the upper 7.5 cm to an initial suction of 9 MPa (RH of 93 %) to account for the accidental opening of the hydration line during the stabilization phase. The initial gas pressure was assumed at the atmospheric pressure of 1 bar. The laboratory temperature of 21.5 °C was set as initial tempera-

Table 1:
Thermal parameters assigned to the insulations and heater device.

Material	Thermal Conductivity [W K^{-1} m^{-1}]	Heat capacity [J kg^{-1} K^{-1}]
Teflon	0.25	960.0
Insulation wool	0.10	1220.0
Insulation foam	0.25	1400.0
Isover	0.10	1000.0
Upper heater device (steel)	52.50	440.0
Lower heater device (insulated)	2.00	440.0
Steel reinforcement (only Exp-B)	52.50	440.0

ture of the whole model domain. Initial saturation is 22% for the Exp-B and 11% for the Exp-SB, according to the available measurements. It is also assumed that there is no initial stress build-up inside the model.

Boundary conditions (BC) are graphically reported in Fig. 2 for the Exp-B case. Except for the mechanical BC, the set-up is the same for the Exp-SB. A no-flow boundary was assigned at the contacts between the filling material, the Teflon and the upper part of the heater device, as the insulation and the steel are hydraulically impermeable. Prior to the hydration phase, no flow was also applied at the upper boundary of the column.

The temperature boundary conditions were assigned directly to the upper and lateral boundaries using the measured laboratory temperature over time. The changes in the insulation set-up during the course of the experiment were reproduced in the models by including the added insulation materials and by shifting the boundary condition for the laboratory temperature accordingly.

Neumann boundary condition were assigned to represent the heating plate by specifying the heating power supplied during the experiment (Fig. 2). Using a heating power controlled boundary condition instead of a specified temperature boundary condition allows for a better estimation of the thermal properties of the filling material. In difference to [9], we did not apply a heat reduction factor to match the measured temperatures, but we could match the measured heater temperature by calibration of the thermal conductivity of the insulation and the heater device materials. Due to the geometrically detailed model set-up, model outputs can be obtained at the same positions as the location of the sensors and the cell load in the experimental set-up, which allows for a valid comparison.

The thermal parameters used in the numerical model are reported in Table 1. The same set of parameters for the insulation set-up was used to simulate both column experiments. The values are derived from literature and they were adjusted within a reasonable range in order to fit the temperature measured on the heater plate and inside the Teflon (Fig. 1b and c).

Buffer material properties

The MX-80 bentonite has long been investigated as buffer material for deep geological radioactive waste disposal, therefore a higher number of measurements is available while less information can be found for the sand-bentonite mixture. THM parameters are listed in Tab. 2 and the applied saturation dependent parameters are explained below.

Table 2:
THM parameters of the filling materials.

	MX-80 bentonite	Sand-bentonite
Porosity [-]	0.444	0.463
Tortuosity [-]	0.8	0.8
Permeability [m^2]	$2.0*10^{-20}$	$1.2*10^{-18}$
Density [g/cm^3]	1530	1450
Poisson coefficient	0.35	Not included
Youngs modulus	$18*10^6$	Not included
Thermal expansion [K^{-1}]	$1.0*10^{-5}$	Not included

Thermal conductivity

[10] and [11] found that the thermal conductivity of the used bentonite strongly depends on the degree of water saturation (as also pointed out by [12] and [13]) while its temperature dependence is negligibly small. For the MX-80, a modified relation from [14] for the saturation dependency of thermal conductivity, which fits the available measurements, was used here (Fig. 3a). Only a limited number of measurements of thermal conductivity are available for the sand-bentonite mixture [11] [4]. Additionally, they are only available for low levels of saturation (Fig. 4a). The thermal conductivity relation used here for the sand-bentonite mixture has higher values (about 0.45 W K^{-1} m^{-1}) at low saturations, as compared to the measurements of about 0.3 W K^{-1} m^{-1} at dry conditions. This higher value is necessary to fit the temperature measured at the sensors. Nevertheless, studies from [15] and [16] indicate that thermal conductivity on the order of 1.2 W m^{-1} K^{-1} are possible for a material of the same density and sand content. Also, the higher thermal conductivity of the sand is the reason why the mixture has been considered as a possible buffer instead of pure bentonite.

Water retention curve

Different relations exist to describe the water retention curve (WRC) of a soil. In our numerical model we used the Van Genuchten relation [17] to match the available suction-saturation measurements. For the MX-80 bentonite, the proposed relation was developed by fitting the van Genuchten relation to the measurements performed at a temperature of 21.5 °C by [18] (Fig. 3b), which are similar to those presented by [19]. The van Genuchten parameters that characterize this curve are a cut-off at $3.0*10^{+11}$ Pa, $\alpha = 1/P_0 = 1*10^{-7}$ Pa^{-1} and $\lambda = 0.237$, with P_0 the entry pressure. For the sand-bentonite mixture the measurements performed by [11] are available only at low saturations. The WRC used in the model (Fig. 4b) was informally provided by J. Rutqvist (Lawrence Berkeley National Laboratory) and was modified to include the few available measurements. The van Genuchten parameters that characterize this curve are a cut-off at $1.0*10^{+9}$ Pa, $\alpha = 1/P_0 = 2.1*10^{-6}$ Pa^{-1} and $\lambda = 0.29$.

Permeability and relative permeabilities

The permeability of both materials was determined by fitting the water intake measured during the Exp-B and Exp-SB experiments. Permeability was considered isotropic and not dependent on changes in porosity. A value of $2.0*10^{-20}$ m^2 was assigned to the MX-80 bentonite, while a value of $1.2*10^{-18}$ m^2 was provided to the sand-bentonite mixture. The relative permeability for water (Kr water) and gas (Kr gas) is dependent on water saturation and the relation used is similar for both the MX-80 and the sand-bentonite mixture. In Fig. 4c only the relation for the mixture is exemplarily reported. These relations have been used to match the relative humidity behavior at the three sensors. A high relative permeability of the water phase is necessary in order to reach the high relative humidity recorded during the hydration phase. Therefore, the used relations show a small permeability at low saturations, but increase strongly when the saturation is approximately 0.35 for the Exp-SB (compare Fig. 4c) and at 0.7 for the Exp-B (not shown). As pointed out in [20] and [21] the relative permeability functions for a material showing a significant bi- or multi-modal pore distribution may deviate significantly from the Van Genuchten-Mualem or Brooks-Corey relations. This effect may lead to increased water flow compared to unimodal pore distributions. The materials investigated both show a bimodal pore distribution, as reported in [22] and [18]. The pore space consists of the pore space in the bentonite pellets as well as the large pores between these pellets. For such a material, water flow will be comparably rapid in the larger pore spaces, leading to fast water transport during the imbibition process [21].

Swelling pressure

The dependency of swelling of the MX-80 bentonite on the increasing saturation was investigated by [23]. The relation used in the numerical model for the Exp-B is shown in Fig. 3c. It deviates from the available measurements by using higher swelling pressures as compared to the measurements at low to intermediate saturations, in order to better fit the axial load pressure measured at the top of the column during the Exp-B.

Results

The following fitting procedure was derived including the outcomes of the sensitivity analysis conducted and used for parameter estimation for the two column experiments. However, due to the high number of parameters for the experimental set-up, results cannot be shown in this report.

First, the thermal parameters of the insulation materials and the cell were obtained by calibration to the temperature measurements at the heater

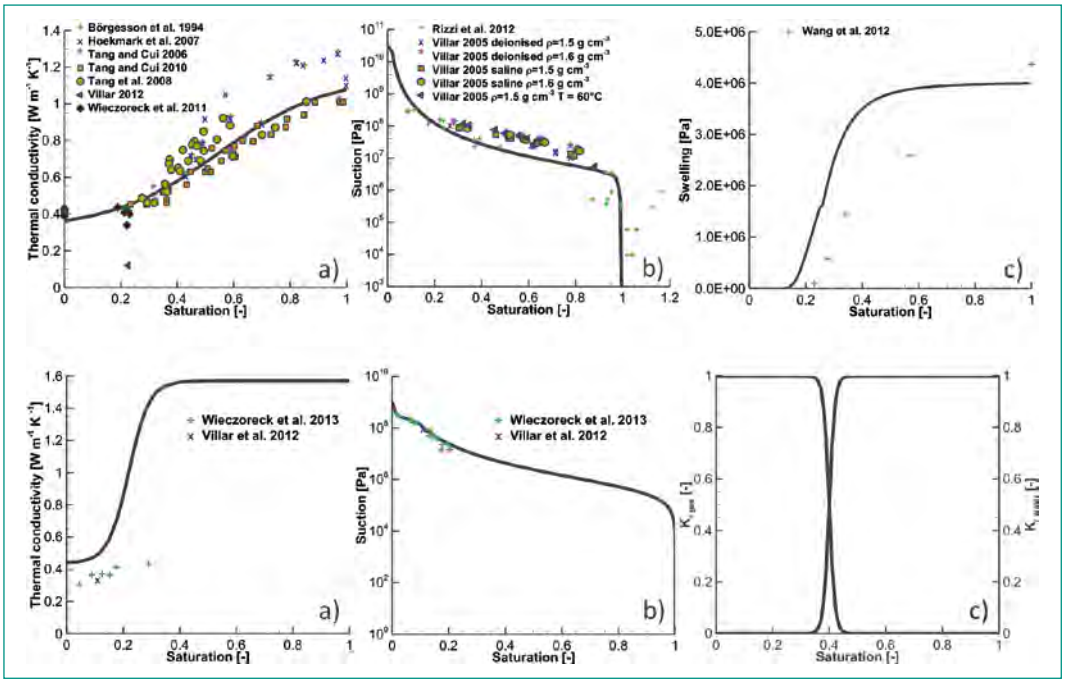

Figure 3 (top): *Relations used for the numerical simulation of Exp-B (black lines) together with the available measurements for a bentonite material of similar characteristics. (a) Thermal conductivity versus saturation; (b) water retention curve; (c) swelling pressure versus saturation.*

Figure 4 (below): *Relations used for the numerical simulation of Exp-SB (black lines) together with the available measurements for the tested sand-bentonite mixtures. (a) Thermal conductivity versus saturation; (b) water retention curve; (c) relative permeability (water and gas) versus saturation.*

plate and inside the Teflon insulation. This was performed for the Exp-B column, and the parameters thus obtained where then transferred to the Exp-SB column, as here the same materials were used. The provided measured temperature variation inside the Teflon [5] is only an average over the last 6000 h of the experiment, therefore its variation is not available and cannot be compared with the model results. The simulated and measured temperatures inside the Teflon are reported in [5]. The numerical results are always slightly lower than the measured temperatures, with a higher discrepancy for Sensor-Teflon2 of around 4 °C in Exp-B. For Exp-SB, differences in Sensor-Teflon1 is less than 1 °C, Sensor-Teflon3 about 3 °C while sensor-Teflon2 shows a difference of around 4 °C. This is considered a good fit, compared to the total temperature span of 20 – 140 °C used in these experiments. Second, the thermal conductivity of the filling materials was determined by fitting to the temperature measurements at Sensors1 through Sensor3. In the third step, the hydraulic behavior of the two columns, i.e. the water intake during the hydration phase and the relative humidity data, was fitted by varying the hydraulic permeability and the relative permeability functions for the two materials. As this causes varying degrees of saturation, a variation in the hydraulic properties makes a reassessment of the determined thermal conductivity necessary, so an iterative approach has to be used. For the Exp-B column, as a last step the axial load was simulated.

Calibration results Exp-B

Results of the calibrated numerical model for the Exp-B column are shown in Fig. 5, where the numerical model results are compared to the temperature, relative humidity, water intake and axial load measurements. The critical parameter for fitting the amount of water intake is the hydraulic permeability, which requires a hydraulic permeability of k = $2.0*10^{-20}$ m² (Fig. 5 c). In a second step, the relative permeability functions were adjusted in order to fit the relative humidity measurements at the three sensors. A relation similar to the one shown in Fig. 4c is used, except that the Kr of water increases at 70 % saturation. The relative humidity evolution for all the sensors can thus be reproduced with good accuracy by the numerical model simulations (Fig. 5a). Deviations occur for the increase in relative humidity at Sensor3 after starting the hydration, which is more pronounced in the measurements, as well as for Sensor1, where relative humidity rises faster in the model than in the experiment (Fig. 5a). The value before hydration and at steady state, i.e. after about 10000 h, are well matched for all sensors.

Temperature at the heater plate is well reproduced by the model for the heating phase, both before and after changes in the insulation set-up with maximum difference of around 5 °C. During the hydration phase, the simulated heater temperature is 5 to 10 °C higher than the measured one. This small deviation is probably caused by an underestimation of the saturation of the bentonite close to the heater, which results in a lower thermal conductivity that affects also the simulated temperature at Sensor3

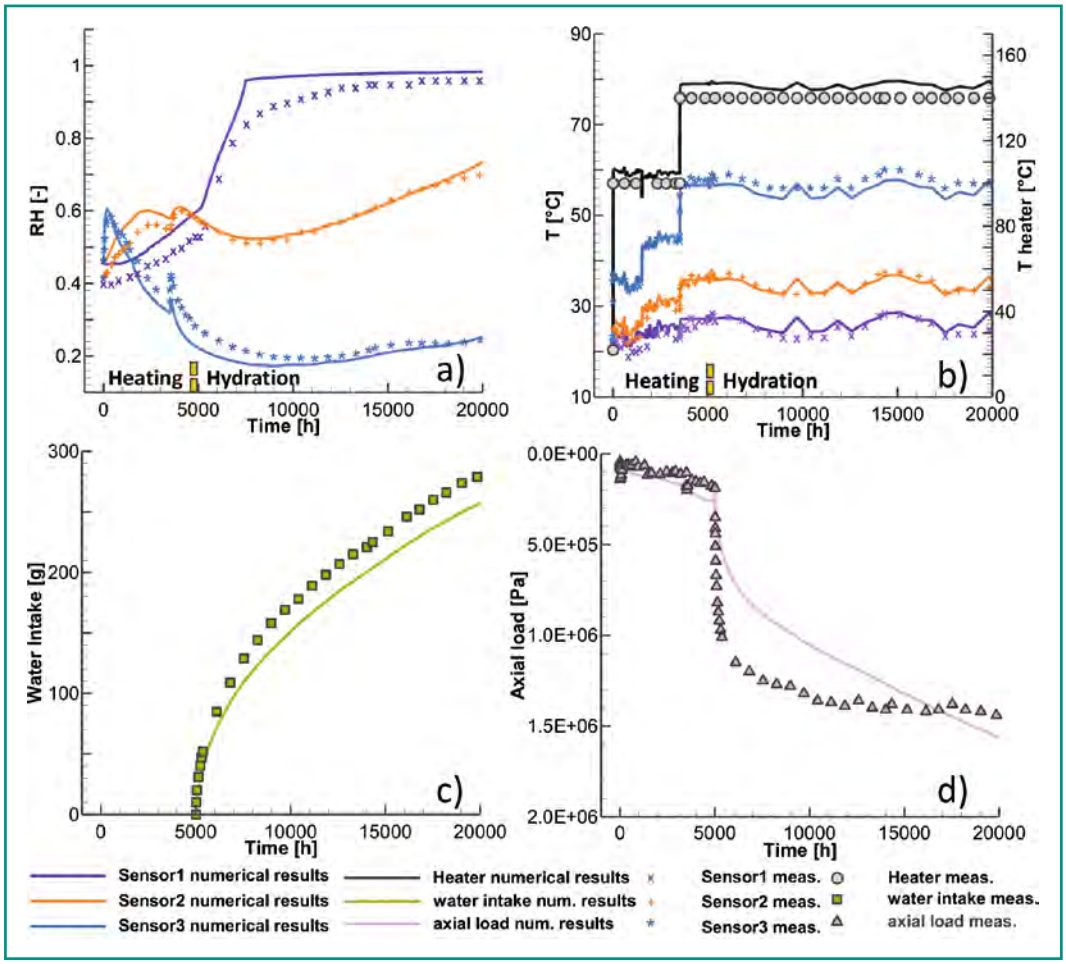

Figure 5:
Simulation results compared to the available measurements for Exp-B. (a) Relative humidity, (b) temperature, (c) water uptake and (d) axial load at the top of the cell. All results are shown versus time.

(Fig. 5b). The overall good match obtained for the temperature evolution indicates that the heat losses calculated laterally through the insulation and through the heater device are correctly approximated with the set of thermal conductivities of the insulation and steel materials and for the used thermal conductivity relation used (Fig. 4a). Fluctuations of the sensor temperatures due to fluctuations in the laboratory temperature are also reproduced satisfactorily, showing that the overall heat balance of the Exp-B column is accurate. The simulation model can also reproduce the trend of the measured axial load for the heating phase. Due to the small changes in water saturation during that phase, changes in axial load are mainly due to thermal expansion of the bentonite pellets. The good fit during the heating phase thus shows that the used thermal expansion of $1.0*10^{-5}$ K^{-1} is correct (Fig. 5d). The simulated axial load during the hydration phase, however, does not reproduce the right time behavior. While the axial load at the end of the experiment is correctly simulated, the simulated rise in axial load is much slower than the measured one, and probably the long term behavior would not be captured correctly (Fig. 5d). This discrepancy is probably due to the linear elastic model used to simulate the swelling effects and also indicates that a different and more appropriate swelling-saturation relation than the one reported in Fig. 3c may be necessary.

Calibration results Exp-SB

For calibration of the Exp-SB sand-bentonite column experiment, the effects of the accidental opening of the hydration line during the stabilization phase had to be included. Therefore, the initial saturation was increased in the upper 7.5 cm of the column from 46 % to 93 %. Only by considering this effect, the relative humidity evolution at Sensor1 and Sensor2 at the beginning of the heating phase can be reproduced (Fig. 6a). The thermal conductivity relation reported in Fig. 4a allows for a good fit of the measured temperatures at the Sensors and at the heater. A thermal conductivity of 0.45 W K^{-1} m^{-1} at dry conditions (Fig. 4a) is required to fit the sensors temperatures during the heating phase, when water saturation is low at about 10–15 % (Fig. 6d). The appropriateness of the thermal conductivity relation used (Fig. 4a) for high saturations is also confirmed by the good fit of temperatures at the heater and the sensors

during the hydration phase at steady state conditions. Only at Sensor2 temperature is underestimated by about 5 °C.

Permeability was fitted using the measured water intake. As shown in Fig. 5c, the value of k = $1.2*10^{-18}$ m^2 used does not allow to reproduce the total water intake measured during the experiment, which is about 900 g. However, at the end of the experiment the Exp-SB column was dismantled and the material weighted to determine the water intake. This measure yielded a water intake of only 700 g, which corresponds to the kink in the measured water intake at about 5000 h. The slow linear increase in water intake after 5000 h is considered as evaporation loss of the column (Dr. Villar, personal communication) therefore the simulation results were calibrated to the water intake of 700 g. This interpretation is also strengthened by the available pore space, as determined by the porosity, which is not large enough to take up 900 g of water. The relative permeability relations were then adjusted to reproduce the relative humidity at the sensors using the relation shown in Fig. 4c. The relations were adapted to reproduce the fast and sharp increase in relative humidity at the beginning of the hydration phase, when all sensors show a relative humidity of 100 % (Fig. 6a) corresponding to a water saturation higher than about 0.5.

International Cooperation

This study was funded by ENSI as part of the DECOVALEX project, which has provided technical support for this study. The experimental data were provided by the partners (CIEMAT, Madrid) of the PEBS project, funded by the European Atomic Energy Community's Seventh Framework Programme (FP7/2007-2011) under grant agreement n° 249681.

Assessment 2015 and Perspectives for 2016

The good fit obtained between the experimental measurements and the numerical results indicates that the developed model succeeded in including the most relevant processes influencing the behavior of the sealing materials around the canister in the early post-closure phase of a HLRW in a deep geological repository. Also, the fact that it is possible to reproduce both experiments using one set of thermal parameters for the buffer material and the insulations provides confidence in the estimation of the relevant parameters and relations for the bentonite and sand-bentonite mixture investigated in the laboratory experiments. Compared to other modelling work from the DECOVALEX project (e.g. [9]), no heat power reduction factor was required to fit the temperature at the heater plate and thus the heat balance is upheld. The developed models can simultaneously fit the thermal and hydraulic effects and, especially at steady state conditions, the fit for both models is satisfactory. The calibration of the developed models could be achieved only by conducting a sensitivity analysis, which determined the most sensitive parameters for the heat and multiphase flow processes. While for the MX-80 bentonite a wide set of measurements (water retention curve, thermal conductivity) are available, thus confirming the correctness of the calibrated parameters, higher uncertainties are associated to the values derived for the sand-bentonite mixture. Additional experimental work characterizing these materials would help to constrain the estimated parameters and their temperature dependence. The materials investigated both show a bimodal pore distribution, as reported in [22] and [18]. The pore space consists of the pore space in the bentonite pellets as well as the large pores between these pellets. For such a material, water

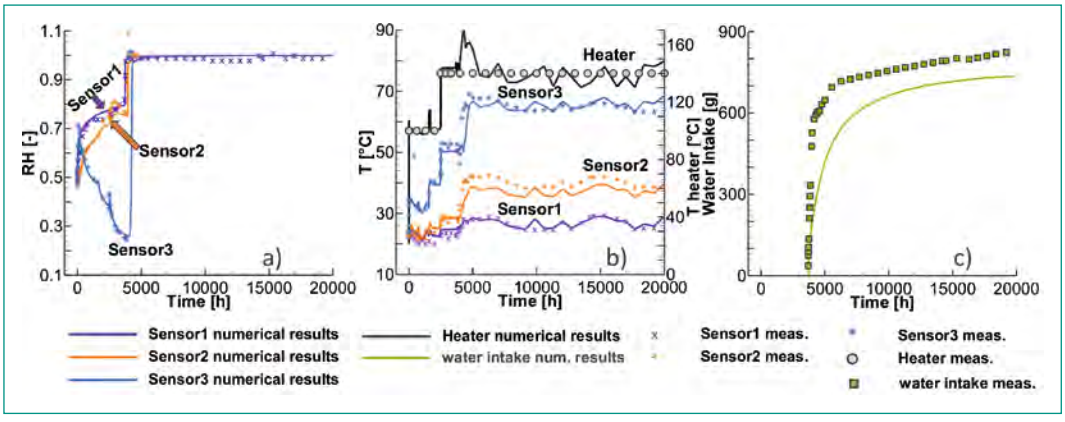

Figure 6: *Numerical results for Exp-SB compared to the available measurements. (a) Relative humidity, (b) temperature, and (c) water intake since the beginning of the hydration phase*

flow will be comparably rapid in the larger pore spaces, leading to fast water transport during the imbibition process [21]. Only by including these effects the fast infiltration of water observed in the experiments can be simulated in the numerical model. While the thermal and hydraulic behavior of the sealing materials is reproduced well by the presented model, further work is required to accurately reproduce the mechanical behavior of the MX-80 bentonite. The purely elastic model combined with thermally induced strain and swelling induced stress does not allow for a satisfactory fit to the measured loads. More complex mechanical material models for the behavior of the bentonite materials have to be employed in order to more accurately represent the induced loads.

Publications

In preparation (for Applied Clay Science): *Ballarini E., Graupner B., Bauer S.* Thermal-hydraulic-mechanical behavior of bentonite and sand-bentonite materials as seal for a nuclear waste repository: Numerical simulation of column experiments.

Abstract and Presentation at the AGU Fall meeting 2015: *Ballarini E., Graupner B., Bauer S.* Thermal-hydraulic behavior of unsaturated bentonite and sand-bentonite material as seal for nuclear waste repository: numerical simulation of column experiments.

References

[1] *Czaikowski O., Garitte B., Gaus I., Gens A., Kuhlmann U., Wieczorek K., 2012.* Design and predictive modelling of the HE-E test. Deliverable (D-N°: 3.2-1) PEBS (Contract Number: FP7 249681) Arbeitsbericht NAB 12-03.

[2] *Gaus I., Wieczorek K., Schuster K., Garitte B., Senger R., Vasconcelos R., Mayor J. C., 2014.* EBS behaviour immediately after repository closure in a clay host rock: HE-E experiment (Mont Terri URL). Geological Society, London, Special Publications doi 10.1144/SP400.11

[3] *Gaus I., Garitte B., Senger R., Gens A., Vasconcelos R., Garcia-Sineriz J. L., Trick T., Wieczorek K., Czaikowski O., Schuster K., Mayor J. C., Velasco M., Kuhlmann U., Villar M. V., 2014.* The HE-E Experiment: Layout, Interpretation and THM Modelling. Arbeitsbericht NAB 14-53.

[4] *Villar M. V., Martín P. L., Gómez-Espina R., Romero F. J., Barcala J. M., 2012.* THM cells for the HE-E test: setup and first results. PEBS Report D2.2.7a. CIEMAT Technical Report CIE MAT/DMA/2G210/02/2012. Madrid, 34 pp.

[5] *Villar M. V., Martín P. L., Romero F. J., 2014.* Long-term THM tests reports: THM cells for the HE-E test: update of results until February 2014. Deliverable-n°: D2.2-7.3. CIEMAT Technical Report IE-MAT/DMA/2G210/03/2014.

[6] *Kolditz O., Bauer S., Bilke L., Böttcher N., Delfs J. O., Fischer T., Görke U. J., Kalbacher T., Kosakowski g., McDermott C. I., 2012a.* OpenGeoSys: an open-source initiative for numerical simulation of thermo-hydro-mechanical/chemical (THM/C) processes in porous media. Environ Earth Sci 67(2):589–599. doi: 10.1007/s12665-012-1546-x

[7] *Kolditz O., Görke U.J., Shao H., Wang W., 2012b.* Thermo-hydromechanical-chemical processes in porous media: benchmarks and examples (lecture notes in computational science and engineering). Springer, Berlin.

[8] *Xie M., Bauer S., Kolditz O., Nowak T., Shao H., 2006.* Numerical simulation of reactive processes in an experiment with partially saturated bentonite. Journal of Contaminant Hydrology, 83 (1–2), 122–147, doi: 10.1016/j.jconhyd.2005.11.003.

[9] *Wang X., Shao H., Wang W., Hesser J., Kolditz O.,* In review. Numerical Modelling of Heating and Hydration Experiments on Bentonite Pellets. Engineering Geology 198 (94–106)

[10] *Wieczorek K., Miehe R., Garitte B., 2011.* Measurement of Thermal Parameters of the HE-E Buffer Materials. Deliverable (D-N°: 2.2-5) PEBS (Contract Number: FP7 249681).

[11] *Wieczorek K., Miehe R., Garitte B., 2013.* Thermal Characterisation of HE-E Buffer. Deliverable (D-N°: 2.2-9) PEBS (Contract Number: FP7 249681).

[12] *Börgesson L., Fredrikson A., Johannesson L. E., 1994.* Heat conductivity of buffer materials, SKB TR-94-29, SKB, Stockholm, Sweden.

[13] *Tang A. M., Cui Y. J., 2006.* Determining the thermal conductivity of compacted MX80 clay, Unsaturated Soils 2006, Reston, Virginia, USA.

[14] *Rutqvist J. and Tsang C.-F., 2004.* A fully coupled 3D THM analysis of the FEBEX in situ test with the ROCMAS code: prediction of the THM behavior in a bentonite barrier. Elsevier

Geo-engineering book series vol.2 2004. Coupled Thermo-Hydro-Mechanical-Chemical processes in geo-systems pp 143–148.

[15] *De Jonge J., Xie M., Kolditz O., 2004.* Numerical implementation of thermally and hydraulically coupled processes in non-isothermal porous media. In: O. Stephansson and John A. Hudson and Lanru Jing (eds.) Coupled Thermo-Hydro-Mechanical-Chemical Processes in Geo-Systems. Elsevier Geo-Engineering Book Series 2:205-210.

[16] *Cho W. J., Lee J. O., Kwon S., 2011*. An empirical model for the thermal conductivity of compacted bentonite and a bentonite-sand mixture. Heat Mass Transfer 47: 1385–1393.

[17] *Van Genuchten MTh. (1980).* A closed-form equation for predicting the hydraulic conductivity of saturated soils. Soil Science Society of American Journal 44: 892–898.

[18] *Rizzi M., Seiphoori A., Ferrari A., Ceresetti D., Laloui L., 2012.* Analysis of the behaviour of the granular MX-80 bentonite in THM-processes. Aktennotiz AN 12-102.

[19] *Villar M. V., 2005.* MX-80 Bentonite.Thermo-Hydro-Mechanical Characterisation Performed at CIEMAT in the Context of the Prototype Project. Informes Técnicos Ciemat 1053 Febrero, 2005. Departamento de Impacto Ambiental de la Energía.

[20] *Durner W., 1994.* Hydraulic conductivity estimation for soils with heterogeneous pore structure. Water Resources Research, Vol. 30, No. 2, pages 211–223.

[21] *Zurmühl T., Durner W., 1998.* Determination of Parameters for Bimodal Hydraulic Functions by Inverse Modeling. Soil Sci. Soc. Am. J. 62:874–880 (1998).

[22] *Rueedi J., Marshall P., Manca D., Ferrari A., Monfared M., Laloui L., Kulenkampff J., Gründig M., Lippmann-Pipke J., Kontar K., 2013.* Arbeitsbericht NAB 12-62 FORGE (fate of Repository Gases) final laboratory report Deliverables D3.34 and D3.36. May 2013.

[23] *Wang Q., Tang A. M., Cui Y. J., Delage P., Gatmiri B., 2012.* Experimental study on the swelling behaviour of bentonite/claystone mixture. Engineering Geology 124 (2012) 59–66. doi: 10.1016/j.engeo.2011.10.003